Title

Quantitative functional characterization of conserved molecular interactions in the active site of mannitol 2-dehydrogenase

Journal

Protein Science, 24(6)

ISSN

0961-8368

Authors

Lucas, James E
Siegel, Justin B

Publication Date

2015-06-01

DOI

10.1002/pro.2669

Peer reviewed

THE PROTEIN SOCIETY

Quantitative functional characterization of conserved molecular interactions in the active site of mannitol 2-dehydrogenase

James E. Lucas[1] and Justin B. Siegel[1,2,3]*

[1]Genome Center, University of California, Davis, California 95616
[2]Department of Chemistry, University of California, Davis, California 95616
[3]Department of Biochemistry & Molecular Medicine, University of California, Davis, California 95616

Received 5 January 2015; Revised 24 February 2015; Accepted 2 March 2015
DOI: 10.1002/pro.2669
Published online 2 April 2015 proteinscience.org

Abstract: Enzyme active site residues are often highly conserved, indicating a significant role in function. In this study we quantitate the functional contribution for all conserved molecular interactions occurring within a Michaelis complex for mannitol 2-dehydrogenase derived from *Pseudomonas fluorescens* (pfMDH). Through systematic mutagenesis of active site residues, we reveal that the molecular interactions in pfMDH mediated by highly conserved residues not directly involved in reaction chemistry can be as important to catalysis as those directly involved in the reaction chemistry. This quantitative analysis of the molecular interactions within the pfMDH active site provides direct insight into the functional role of each molecular interaction, several of which were unexpected based on canonical sequence conservation and structural analyses.

Keywords: enzyme; mannitol 2-dehydrogenase; mutagenesis; molecular; interactions; conserved; catalysis; binding; specificity; quantitative

Introduction

Investigating the functional role of molecular interactions within enzyme active sites is critical to our understanding of how enzymes are able to achieve unparalleled levels of specificity and catalytic proficiency.[1–3] To date, most functional studies on the role of active site residues in enzymes have focused on molecular interactions directly involved in reaction chemistry.[1,4–6] These studies have led to an in-depth understanding on how enzymes carry out chemical reactions and the flow of electrons and protons within active sites.[7–10] However, active site residues that are not directly involved in the reaction chemistry are rarely assessed for their role in enzyme function. Yet, these residues are often highly conserved, indicating that they may also play an important role in enzyme function.[11,12] A systematic experimental study quantitating the contribution of highly conserved active site residues towards an enzyme's catalytic parameters, including both catalytic residues and those not predicted to be directly involved in reaction chemistry, has yet to be performed. Here we quantitatively characterize the functional role of all the conserved residues within an enzyme active site to elucidate each residue's role in catalysis and specificity.

The enzyme focused on in this study is pfMDH (E.C. 1.1.1.67, UniProt Accession #: O08355). This enzyme is an NAD^+ dependent secondary alcohol dehydrogenase that catalyzes the reversible oxidation of polyols such as D-mannitol (Fig. 1). Significant structural and mechanistic studies have been carried out on this enzyme because of its industrial significance in the conversion of D-fructose to D-mannitol, a diuretic used to treat cystic fibrosis and aid

Abbreviations: BSA, bovine serum albumin; HEPES, 4-(2-hydroxyethyl)−1-piperazineethanesulfonic acid; MWCO, molecular weight cut-off; NAD, nicotinamide adenine dinucleotide; PBS, phosphate buffered saline; pfMDH, *Pseudomonas fluorescens* mannitol 2-dehydrogenase; WT, wild type

Additional Supporting Information may be found in the online version of this article.

*Correspondence to: Justin B. Siegel; 451 Health Sciences Drive, Room 1315 | Davis, CA 95616. E-mail: jbsiegel@ucdavis.edu

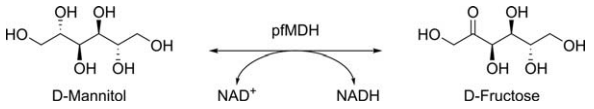

Figure 1. Native reaction catalyzed by pfMDH. An NAD^+ cofactor is utilized to reversibly oxidize the secondary alcohol of D-mannitol and yield D-fructose.

in the transport of drugs across the blood-brain barrier.[13,14] D-mannitol is also a common additive to chewing gum as a sugar substitute and is used as an excipient in pharmaceutical applications.[15,16]

Structures of pfMDH are available in the binary complex with NADH (PDB-ID: 1LJ8) as well as the ternary complex with NADH and D-mannitol (PDB-ID: 1M2W). A structural alignment of the ternary and binary forms does not reveal any significant structural rearrangement in either the overall ternary structure or in the molecular details of the active site (Fig. 2). We therefore hypothesized that pfMDH functions primarily through a lock-and-key based mechanism, for which both catalysis and specificity are primarily dictated by the direct molecular interactions between enzyme and substrate within the active site. This apparent lack of large conformational changes makes pfMDH a good model system for characterizing how molecular interactions within an enzyme active site affect catalysis and substrate specificity.

Previous efforts in characterizing the molecular interactions within the active site of pfMDH have led to a proposed reaction mechanism (Fig. 3). This mechanism is supported by mutagenesis data in which key molecular interactions predicted to be involved in the reaction chemistry were removed, resulting in a 300 to 400,000 fold decrease in activity at pH 10.[17] Removal of Lys295, a primary catalytic residue which serves as a proton acceptor in the catalytic mechanism, results in a 400,000-fold decrease in catalytic efficiency as compared to wild type (WT) pfMDH. Removal of His303 and Asn300 cause 300-fold and 1000-fold decreases in catalytic efficiency, respectively.[17] Further experimental investigations of the functional importance for the remaining active site residues have yet to be carried out.

In this study we systematically engineer a series of pfMDH mutants in which molecular interactions between D-mannitol and pfMDH are removed. Kinetic constants were measured for each mutant under standardized neutral conditions to determine the interaction's role in turnover rate (i.e. k_{cat}). Furthermore, each enzyme was kinetically characterized against a series of polyol and hexanol substrates of varying chain length and alcohol composition. The kinetic data obtained from the pfMDH mutants and selected substrates help further our understanding of how molecular interactions in the active site affect enzyme catalysis and substrate specificity.

Results

Identification of relevant active site residues

The ternary structure of pfMDH with D-mannitol and NADH bound (PDB-ID: 1M2W) was used to identify residues making molecular interactions with D-mannitol in the active site. Active site residues with atoms within 3.5 Å of D-mannitol were considered to be making molecular interactions of significant interest (Fig. 2). The previously proposed catalytic mechanism for pfMDH was referenced to classify active site residues directly involved in oxidation of the C_2 alcohol of D-mannitol.[18] Three catalytic residues were identified: Asn191, Lys295, and Asn300 (Fig. 2). Five

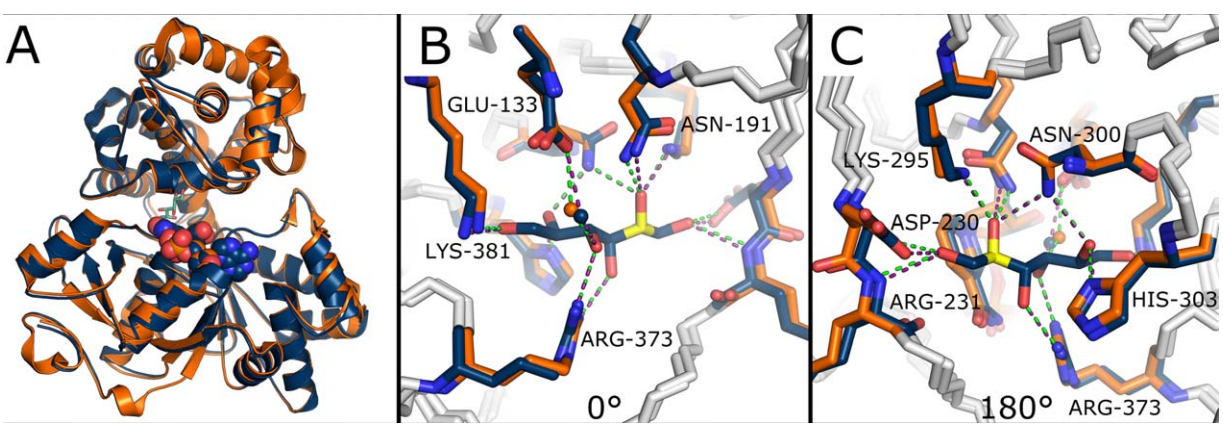

Figure 2. Overlay of the binary (1LJ8; orange) and ternary (1M2W; dark blue) structures of pfMDH where no large structural rearrangement occurs when D-mannitol is bound. (A) The structures have a Cα-RMSD of 0.7 Å. NAD is shown in spheres and D-mannitol is depicted in teal. (B) Active site overlay of the binary and ternary structures of pfMDH. There is no substantial conformational change in active site residues between the binary and ternary structures. Hydrogen bonds between 1LJ8 and D-mannitol are shown in green while interactions between 1M2W and D-mannitol are shown in purple. The C_2 carbon of D-mannitol is shown in yellow and water is represented as spheres. (C) Rear projection of Figure 2(B). Figures were made with PyMol version 1.703.[27]

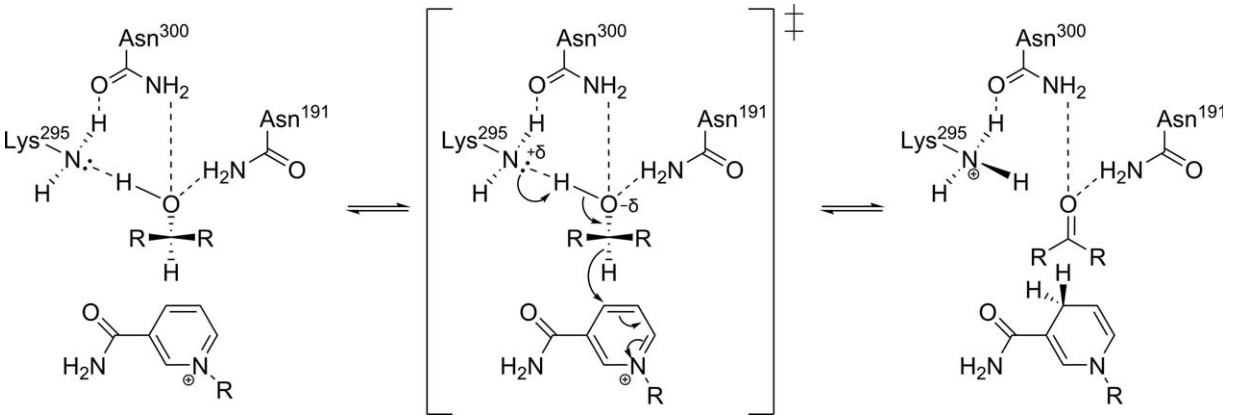

Figure 3. Proposed reaction mechanism for pfMDH where Asn191 and Asn300 create stabilizing hydrogen bonding interactions with Lys295 and the substrate. Lys295 serves as a proton acceptor while NAD^+ facilitates a hydride transfer.[18]

residues in the active site maintain molecular interactions with D-mannitol but are not directly involved with the reaction chemistry: Glu133, Asp230, His303, Arg373, and Lys381. Where Asp230, His303, Arg373, and Lys381 are in direct contact with D-Mannitol through hydrogen bonding, Glu133 is involved in creating a water bridge between the enzyme and the substrate (Fig. 2).

To further support the importance of these residues, we assessed their level of conservation within the MDH enzyme family. A HMMER[19] search of the UniProtKB[20] was used to identify sequence homologs. This set was further curated using CD-HIT[21] to remove redundant sequences at a cutoff of 80%. Sequences were then curated for length in which only sequences within 10% of the overall pfMDH length were kept. This procedure resulted in a set of 184 nonredundant sequences ranging between 36% and 80% in sequence identity to pfMDH (accession numbers in Supporting Information Table S1). A multiple sequence alignment generated using MUSCLE[22] confirmed the predicted importance of the residues that had been identified based on our structural analysis. A sequence logo of the region around each of the residues illustrates their level of conservation in Figure 4. The residues predicted to be involved in reaction chemistry are 100% conserved among the MDH enzyme family. Residues 191 and 300 are 100% conserved as asparagine while residue 295 is 100% conserved as lysine. Residues not directly involved in the reaction chemistry were also found to maintain a high degree of conservation. Residue 230 is 100% conserved as aspartic acid and residue 303 is 100% conserved as histidine across all sequences. Residue 133 and 373 are both >99% conserved as glutamate or arginine, respectively. Residue 381 had lower conservation in terms of identity as a lysine, but the observed amino acid is 98% conserved as either lysine or arginine. Due to high conservation over a highly diverse set of sequences, and observed interactions with D–mannitol, we hypothesized that these residues would play a critical role in the pfMDH reaction and warranted further investigation. We also hypothesized that the catalytic residues in direct contact with the C_2 alcohol of D–mannitol would primarily affect the turnover rate, and that residues not directly interacting with the C_2 alcohol would primarily affect the substrate binding and specificity. To test these hypotheses we engineered a series of pfMDH mutants and measured their kinetic constants against a series of substrates.

Residues directly involved in the reaction chemistry

The N191A and K295A mutations were engineered to remove hydrogen bond interactions with the C_2 alcohol of D–mannitol (Fig. 2). Removing Asn191 decreases turnover rate to 0.02 s^{-1}, a 220-fold decrease in k_{cat}. This mutation also decreases K_M to 4.6 m*M*, a 30% decrease as compared to WT pfMDH (Table I). Asn191 is found to contribute 3.0 kcal/mol to catalytic efficiency, with 3.2 kcal/mol towards k_{cat} and −0.2 kcal/mol from K_M (Fig. 5). The elimination of Lys295 results in no detectable activity under our assay conditions, representing a >734,000-fold decrease in enzyme activity (Table I).

The N300A and N300S mutations were engineered to remove two hydrogen bond interactions with the C_2 and C_5 alcohols of D–mannitol (Fig. 2). In addition, N300D was introduced as an isosteric mutant to determine the importance of the amide group in creating hydrogen bond interactions with D–mannitol. Both N300A and N300S result in similar decreases in k_{cat}, reducing the turnover rate to 0.21 s^{-1} (21-fold decrease) and 0.10 s^{-1} (46-fold decrease), respectively. N300A possesses a K_M of 69.0 m*M* (12-fold increase) while N300S possesses a K_M of 50.0 m*M* (8-fold increase, Table I). The N300A mutation results in a 3.2 kcal/mol decrease in catalytic efficiency, with 1.8 kcal/mol from k_{cat} and 1.4 kcal/mol from K_M (Fig. 5). The N300S decreases catalytic efficiency by 3.5 kcal/mol, with 2.3 kcal/mol from

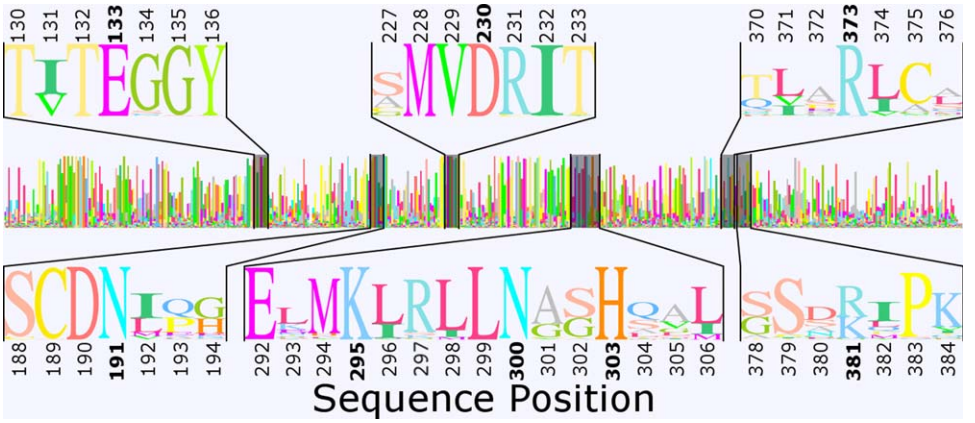

Figure 4. Sequence logo representing 184 diverse sequences that are homologous to pfMDH. The active site regions are highlighted and residue numbering corresponding to pfMDH is depicted, Residues N191, D230, K295, N300, and H303 are 100% conserved. Where E133 and R373 are >99% conserved in the MDH enzyme family, K381 is 98% conserved as either lysine or arginine.

k_{cat} and 1.3 kcal/mol from K_M (Fig. 5). The N300D mutation results in a 5,289-fold decrease in k_{cat} with a turnover rate of 8.3×10^{-4} s^{-1}. This mutation increases the K_M to 20.4 m*M*, a three-fold increase as compared to WT pfMDH (Table I). The N300D mutation causes a 0.7 kcal/mol increase in K_M and 5.1 kcal/mol decrease in k_{cat}, a total contribution of 5.8 kcal/mol to catalytic efficiency (Fig. 5).

Residues not directly involved in the reaction chemistry

The D230A mutation was designed to eliminate the hydrogen bond interaction with the C_1 alcohol of D–mannitol (Fig. 2). As compared to WT pfMDH, removing this residue results in an 11-fold decrease in turnover rate to 0.39 s^{-1} and a seven-fold increase in K_M to 42.7 m*M* (Table I). Asp230 contributes 2.6 kcal/mol to catalytic efficiency, with 1.4 kcal/mol from k_{cat} and 1.2 kcal/mol from K_M (Fig. 5).

Table I. *Kinetic Constants for WT and Mutant pfMDH on D-Mannitol*[a]

Enzyme	k_{cat} (s^{-1})	K_M (m*M*)	k_{cat}/K_M ($M^{-1}s^{-1}$)
WT	4.39 ± 0.11	5.98 ± 0.67	734.25 ± 84.83
E133A	3.99 ± 0.07	18.21 ± 1.13	219.04 ± 14.22
E133Q	3.22 ± 0.09	14.96 ± 1.50	215.07 ± 22.34
N191A	0.0209 ± 0.0002	4.56 ± 0.24	4.58 ± 0.25
D230A	0.39 ± 0.17	42.74 ± 4.94	9.08 ± 1.12
K295A	ND	ND	ND
N300A	0.21 ± 0.01	68.94 ± 5.80	3.11 ± 0.28
N300D	0.00083 ± 0.00007	20.42 ± 5.48	0.04 ± 0.01
N300S	0.096 ± 0.006	49.95 ± 7.88	1.92 ± 0.33
H303A	0.49 ± 0.04	93.85 ± 14.64	5.22 ± 0.90
R373A	0.0180 ± 0.0005	17.49 ± 1.74	1.02 ± 0.11
K381A	0.190 ± 0.002	23.89 ± 0.69	7.75 ± 0.23
H303A+ R373A+ K381A	0.0010 ± 0.0004	8.15 ± 1.07	0.16 ± 0.02

[a] Kinetic data calculated from eight data points obtained in triplicate by measuring the accumulation of NADH at a wavelength of 340 nm during the oxidation of D-mannitol over the period of an hour. Assay was performed in 100 μL 50 m*M* HEPES with 150 m*M* NaCl (pH 7.4), 1 mg/mL BSA, 1 m*M* NAD^+, and 90–900 n*M* pfMDH. Two-fold serial dilutions were performed on the substrate where the maximum final concentration of D-mannitol was 200 m*M*. ND = No detection, detection limit of 0.001 $M^{-1}s^{-1}$.

The H303A mutation was engineered to remove a hydrogen bond interaction with the C_5 alcohol of D–mannitol (Fig. 2). The removal of this interaction results in a 16-fold increase in K_M for pfMDH, from 5.98 to 93.9 m*M*. The removal of this interaction decreases the turnover rate nine-fold, from 4.4 to 0.5 s^{-1} (Table I). Therefore, His303 provides 2.9 kcal/mol towards catalytic efficiency, with 1.6 kcal/mol from K_M and 1.3 kcal/mol from k_{cat} (Fig. 5).

The R373A mutation was introduced to remove hydrogen bond interactions with the C_3 and C_4 alcohols of D–mannitol (Fig. 2). The removal of the two hydrogen bonds between the guanidino group of Arg373 and D–mannitol results in a K_M of 17.5 m*M*, a three-fold increase. This mutation results in a 247-fold decrease in k_{cat}, with a turnover rate of 0.02 s^{-1} (Table I). Overall, Arg373 is measured to contribute 3.9 kcal/mol towards catalytic efficiency, with 0.6 kcal/mol towards K_M and 3.3 kcal/mol towards k_{cat} (Fig. 5).

The K381A mutation was engineered to remove a hydrogen bond with the C_6 alcohol of D–mannitol (Fig. 2). The removal of this interaction results in a four-fold increase in K_M to 23.9 m*M*. The removal of this interaction also causes a 24-fold decrease in k_{cat}, resulting in a turnover rate of 0.2 s^{-1} (Table I). Overall, Lys381 is measured to contribute 2.7 kcal/mol to catalytic efficiency, with 1.9 kcal/mol towards k_{cat} and 0.8 kcal/mol towards K_M (Fig. 5).

A triple mutant (H303A, R373A, and K381A) was designed to remove the direct molecular interactions between the C_3–C_6 alcohols of D–mannitol and the residues from pfMDH not directly involved in

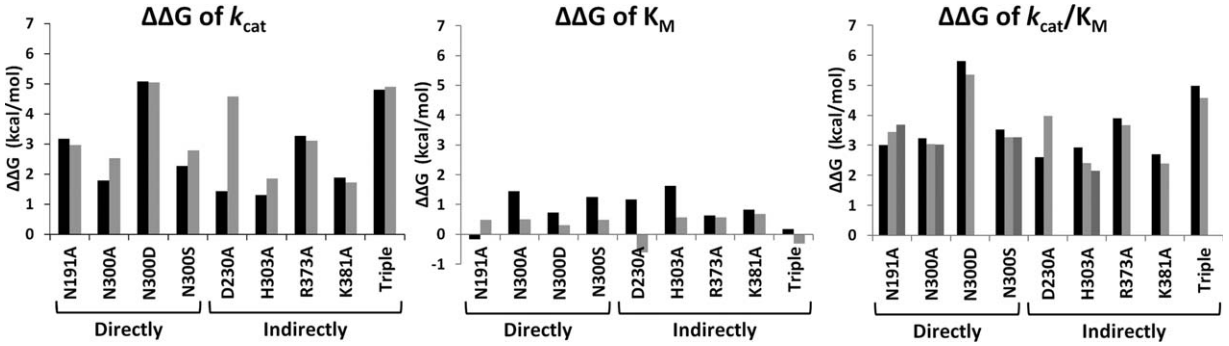

Figure 5. Energetic changes of the measured kinetic constants between WT pfMDH and selected mutants on D-mannitol (black), D-arabitol (light gray), and meso-erythritol (dark gray). Residues are grouped as directly or indirectly involved in catalysis. Mutant labeled "Triple" is the triple mutant containing the H303A, R373A, and K381A mutations. Changes in free energy were calculated using the first order Arrhenius equation (Equation and constants provided in Supporting Information Fig. S5).

catalysis (Fig. 2). Removing the four hydrogen bond interactions with D–mannitol results in a K_M of 8.15 m*M*, less than a two-fold increase in K_M. While the removal of these interactions has a relatively small effect on K_M, this mutant causes a 3,377-fold decrease in k_{cat} with a turnover rate of 1.3×10^{-3} s^{-1} (Table I). The combined effect of these residues contributes 5.2 kcal/mol towards catalytic efficiency, with 5.0 kcal/mol towards k_{cat} and 0.2 kcal/mol towards K_M (Fig. 5).

Mutant E133A was engineered to disrupt the water bridge interacting with the C_4 alcohol of the D–mannitol substrate (Fig. 2). In addition to E133A, E133Q was introduced as an isosteric mutant to determine the importance of the negative charge contributed by the glutamate residue. Both mutations result in a three-fold decrease in K_M. The mutation E133A has a K_M of 15.0 m*M* while E133Q possesses a K_M of 18.2 m*M*. Both mutations result in less than a 25% decrease in turnover rate where E133A has a k_{cat} of 3.2 s^{-1} and E133Q has a k_{cat} of 4.0 s^{-1} (Table I). The effects of E133A and E133Q on the kinetic constants of pfMDH suggest that the water bridge mediated by Glu133 and the negative charge of the glutamate residue do not play a significant role in catalysis, an unexpected result given the high degree of sequence conservation at this position.

Substrate specificity of WT pfMDH and mutants

We proceeded to assay the WT and mutant pfMDHs against several polyol substrates to characterize differences in catalytic activity (Fig. 6). The polyol substrates tested were D–arabitol, meso-erythritol, and glycerol, essentially starting from D–mannitol and systematically removing one carbon at a time. To determine whether solvation plays a role in catalysis both 1,2-hexanediol and 1,2,3-hexanetriol were also assayed against WT and mutant pfMDH.

Of the substrates assayed, WT and mutant pfMDHs demonstrate detectable activity on D–arabitol and meso-erythritol. Wild-type pfMDH is measured to have a K_M of 55.8 m*M* and a k_{cat} of 6.6 s^{-1} on D–arabitol (Table II), with a catalytic efficiency of 118.0 $M^{-1}s^{-1}$. For meso-erythritol no detectable substrate saturation is observed, but WT pfMDH is measured to have a catalytic efficiency of 64.7 $M^{-1}s^{-1}$ on meso-erythritol (Table III). The overall trends for the functional effects of the mutants on D–arabitol and meso-erythritol are highly similar to what is observed for D–mannitol (Fig. 5). However, a few mutants demonstrated significant and unexpected differences in function on D–mannitol, D–arabitol and meso-erythritol.

Mutants with unexpected effects on D–arabitol

The D230A mutant possesses a significantly lower turnover rate for D–arabitol as compared to D–mannitol. Where D230A causes an 11-fold decrease in turnover rate on D–mannitol, there is a 2,288-fold decrease in turnover rate on D–arabitol. This translates to a 1.2 kcal/mol contribution to k_{cat} on D–mannitol and a 4.6 kcal/mol contribution to k_{cat} by Asp230 on D–arabitol (Fig. 5). The D230A mutant also decreases K_M two-fold from 55.8 to 20.4 m*M* as compared to WT pfMDH. This simultaneous decrease in K_M and turnover rate in the absence of Asp230 suggests that this residue plays an essential role in correctly positioning the secondary alcohol of the substrate for catalysis.

Since D–arabitol lacks the additional C_6 alcohol which D–mannitol possesses, we expected that the K381A mutant would have a minimal effect on the kinetic constants of pfMDH in the catalysis of D–arabitol. Even though no expected protein-substrate interactions were altered between WT pfMDH and the K381A mutant when D–arabitol is the substrate, this mutation causes an increase in K_M and decrease in k_{cat} comparable to mutated residues that do make direct contact with D–arabitol. Furthermore, the relative effects of WT pfMDH versus the K381A mutant on D–arabitol and D–mannitol are observed to be equivalent.

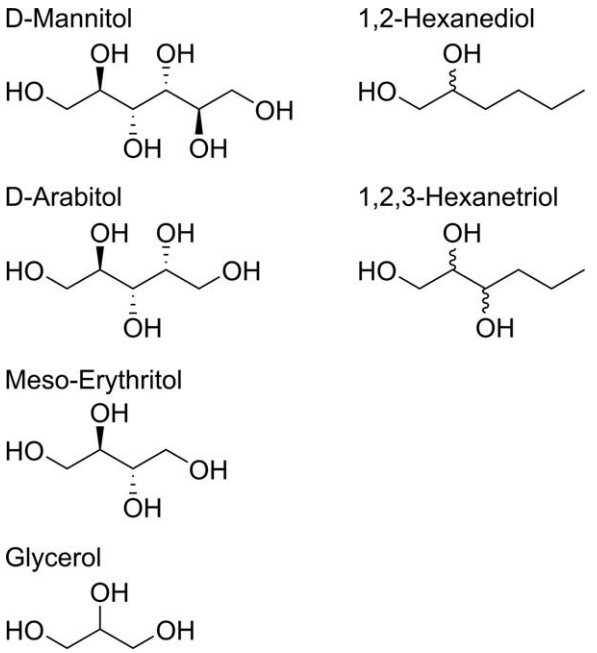

Figure 6. Skeletal formulas of the substrates used to investigate the specificity of WT and mutant pfMDHs.

Mutants with unexpected effects on meso-erythritol

None of the mutants were observed to saturate up to 1.8*M* meso-erythritol, and therefore our analysis is limited to overall catalytic efficiency. While energetic contributions towards catalysis for each residue are generally consistent with D–arabitol and D–mannitol (Fig. 5), it was unexpected that the K381A mutant does not have detectable activity on meso-erythritol. For both D–arabitol and D–mannitol roughly a 100-fold decrease in catalytic efficiency is observed for K381A. For meso-erythritol a 100-fold decrease would still be well within our detection limit for activity.

Glycerol

Neither WT nor mutant pfMDH enzymes possess detectable activity on glycerol. Reactions were set up with 10 μ*M* enzyme and monitored for an hour at 200 m*M* substrate concentration, during which a single turnover would have been readily detected. However, no substrate oxidation was observed. Therefore the enzymes have a catalytic efficiency of less than 0.001 M^{-1} s^{-1} on this potential substrate. For WT pfMDH, this represents >4.7 kcal/mol change in activation energy from the loss of a single alcohol in the polyol. We hypothesized that the short chain length of glycerol could allow for alternative, nonproductive, binding modes in the active site. To investigate this hypothesis, an inhibition assay was conducted with D–mannitol and glycerol on WT pfMDH. We anticipated competitive inhibition of D–mannitol if glycerol was able to bind anywhere in the pfMDH active site. However, with up to 10% (1.1*M*) glycerol there was no significant inhibition observed over a range of D–mannitol concentrations, ranging from subsaturating to saturation (Fig. 7).

Table II. *Kinetic Constants for WT and Mutant pfMDH on D-Arabitol*[a]

Enzyme	k_{cat} (s^{-1})	K_M (m*M*)	k_{cat}/K_M ($M^{-1}s^{-1}$)
WT	6.59 ± 0.36	55.85 ± 7.54	118.00 ± 17.17
E133A	7.30 ± 0.25	134.06 ± 8.78	54.48 ± 4.04
E133Q	5.50 ± 0.14	126.92 ± 6.37	43.32 ± 2.45
N191A	0.044 ± 0.001	125.46 ± 7.50	0.35 ± 0.02
D230A	0.0029 ± 0.0002	20.36 ± 4.35	0.14 ± 0.03
K295A	ND	ND	ND
N300A	0.092 ± 0.006	132.11 ± 9.61	0.69 ± 0.06
N300D	0.0013 ± 0.0001	94.82 ± 20.06	0.014 ± 0.003
N300S	0.060 ± 0.004	126.53 ± 14.66	0.47 ± 0.06
H303A	0.29 ± 0.01	145.12 ± 6.65	2.00 ± 0.10
R373A	0.034 ± 0.003	144.46 ± 23.96	0.24 ± 0.04
K381A	0.37 ± 0.01	176.87 ± 6.55	2.06 ± 0.09
H303A+ R373A+ K381A	0.0017 ± 0.0001	33.15 ± 9.00	0.051 ± 0.015

[a] Kinetic data calculated from eight data points obtained in triplicate by measuring the accumulation of NADH at a wavelength of 340 nm during the oxidation of D-arabitol over the period of an hour. Assay was performed in 100 μL 50 m*M* HEPES with 150 m*M* NaCl (pH 7.4), 1 mg/mL BSA, 1 m*M* NAD+, and 90–900 n*M* pfMDH. Two-fold serial dilutions were performed on the substrate where the maximum final concentration of D-arabitol was 200 m*M*. ND = No detection, detection limit of 0.001 $M^{-1}s^{-1}$.

1, 2-Hexanediol and 1, 2, 3-hexanetriol

One potential hypothesis for the $>C_3$ polyol specificity of pfMDH is through a substrate-assisted

Table III. *Kinetic Constants for WT and Mutant pfMDH on Meso-Erythritol*[a]

Enzyme	k_{cat} (s^{-1})	K_M (*M*)	k_{cat}/K_M ($M^{-1}s^{-1}$)
WT	>0.599	>>1.8	1.08 ± 0.04
E133A	>0.538	>>1.8	0.97 ± 0.02
E133Q	>0.489	>>1.8	0.88 ± 0.01
N191A	>0.0012	>>1.8	0.0021 ± 0.0002
D230A	ND	ND	ND
K295A	ND	ND	ND
N300A	>0.0036	>>1.8	0.0065 ± 0.0003
N300D	ND	ND	ND
N300S	>0.0024	>>1.8	0.0044 ± 0.0003
H303A	>0.0159	>>1.8	0.029 ± 0.002
R373A	ND	ND	ND
K381A	ND	ND	ND
H303A+ R373A+ K381A	ND	ND	ND

[a] Kinetic data calculated from eight data points obtained in triplicate by measuring the accumulation of NADH at a wavelength of 340 nm during the oxidation of meso-erythritol over the period of an hour. Assay was performed in 100 μL 50 m*M* HEPES with 150 m*M* NaCl (pH 7.4), 1 mg/mL BSA, 1 m*M* NAD+, and 0.4–4 μ*M* pfMDH. Two-fold serial dilutions were performed on the substrate where the maximum final concentration of meso-erythritol was 1.8*M*. ND = No detection, detection limit of 0.001 $M^{-1}s^{-1}$.

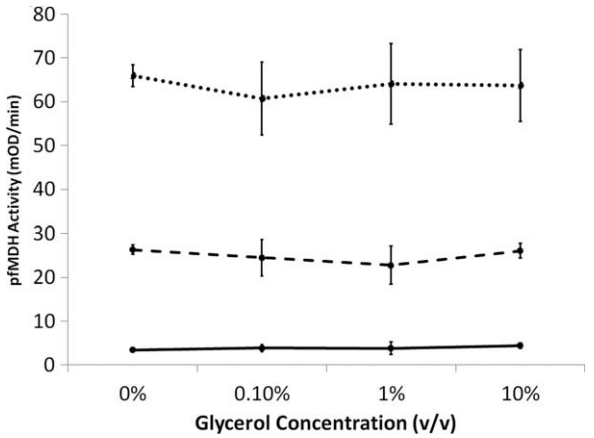

Figure 7. Effect of glycerol on the catalysis of pfMDH with 100 m*M* (dots), 10 m*M* (dashes), or 1 m*M* (solid) D-mannitol. Each assay was done in triplicate and error bars represent the standard deviation.

mechanism in which the extended substrate chain occludes the catalytic center from the solvent, changing the electrostatic potential of the reaction center. To investigate this possibility we assayed 1, 2-hexanediol and 1, 2, 3-hexanetriol, both as mixtures of stereoisomers, against WT and mutant pfMDH to determine the role of solvation in the catalytic mechanism of this enzyme. These substrates would maintain the occlusion of the reaction center from solvent, but would not provide the hydroxyls for binding. The substrate 1,2,3-hexanetriol was of particular interest for the triple mutant (Fig. 6) as the molecular interactions between the mutant on D–mannitol and 1,2,3-hexanetriol are predicted to be identical except for the hydrogen bond made between Asn300 and the C_2 alcohol of D–mannitol. However, even at 10 μ*M* protein and 20 m*M* substrate concentration there is no observed oxidation over an hour period.

Discussion

The quantitative analysis of WT and mutant pfMDH enzymes on polyols of varying chain lengths has revealed that the molecular interactions throughout the entire Michaelis complex are important for enzyme catalysis, and in particular the turnover rate. Our investigation supports the currently accepted reaction mechanism and reveals that this enzyme possesses substrate specificity for polyols greater than three carbons in length. We have also identified several highly conserved active site residues which play unexpected roles in catalysis.

The substantial decrease in catalytic activity on D–mannitol when the interactions created by Lys295, Asn191, and Asn300 are removed is consistent with these residues' involvement in the currently proposed reaction mechanism. Eliminating Lys295, the crucial proton acceptor in the proposed reaction mechanism, results in an enzyme with no detectable activity in our assay conditions. Removing Asn191, which creates a hydrogen bond interaction with the C_2 alcohol of D–mannitol, results in a 210-fold decrease in turnover rate. The Asn300 mutants also demonstrate the critical role this residue plays in the reaction chemistry. Most notably, the isosteric N300D mutation results in a 5,289-fold decrease in the turnover rate. This suggests that the hydrogen bonding interactions between the amide group of Asn300 and the C_2 and C_5 alcohols of D–mannitol are critical to catalysis. Given the close proximity of residue 300 to Lys295, this decrease in activity may also be attributed to a salt bridge created between Lys295 and Asp300; a salt bridge would stabilize the positive charge on the catalytic lysine and decrease its ability to accept the hydrogen from the C_2 alcohol of a substrate.

While previous studies had not elucidated the role of the remaining residues in the active site, we demonstrate that most of the residues are critical for catalysis, specifically the turnover rate. The exception to this observation is Glu133, where the removal of the water bridge interaction between this residue and the C_4 alcohol of D–mannitol has a negligible effect on k_{cat}. It is possible that water reorients itself to maintain hydrogen bonding interactions between the several nearby polar residues and the C_4 alcohol of D–mannitol. While it is now clear that this residue does not play a role in pfMDH enzyme catalysis, it may play a role in substrate specificity. In this study we assessed specificity in terms of polyol chain length; however, there are many additional potential substrates in a cellular environment.

One of the most significant, and unexpected, functional contributions towards catalysis came from Asp230 on D–arabitol. Even though it is not involved in the reaction chemistry, replacing Asp230 with alanine produces an effect comparable to removing the catalytic residues Asn191 and Asn300. The drastic change in turnover rate when Asp230 is removed indicates that this residue is vital for properly positioning the secondary alcohol of the substrate in the active site for catalysis to occur.

Based on the ternary structure pfMDH, the functional effect of Lys381 on D–arabitol and meso-erythritol was also unexpected. Unlike D–mannitol, Lys381 is not expected to be making a direct molecular interaction for these two substrates, and therefore the mutation to alanine was expected to have a minimal effect on catalysis. However, this mutation causes an 18-fold decrease in turnover rate on D–arabitol and >600-fold decrease on meso-erythritol. We propose that this supports a role for the positive charge of Lys381 in the enzyme catalyzed reaction, yet further mechanistic and biophysical studies are needed to elucidate how the positive charge is playing a role in enzyme catalysis.

We have found that pfMDH exhibits substrate specificity towards polyols greater than three carbons in length. There is less than a 10-fold decrease

in catalytic efficiency observed for WT and mutant pfMDHs when comparing D–mannitol versus D–arabitol, and a 100-fold decrease when comparing D–arabitol versus meso-erythritol. However, when comparing meso-erythritol versus glycerol there is greater than a 1000-fold decrease in activity. No competitive binding is observed during glycerol inhibition assays, suggesting that glycerol is not simply binding in a non-productive mode in our assay conditions. Based on the structure there is no obvious reason why the change from meso-erythritol to glycerol would result in a functional effect corresponding to 4.1 kcal/mol. As hydrogen bonds for peptides are often considered to provide 1.0–1.5 kcal/mol, with the highest reports in solution being ~7.8 kcal/mol, this indicates that the C_4 alcohol is making a strong hydrogen bond and plays a critical role in enzyme catalysis for pfMDH.[23,24]

In summary, we have quantitatively characterized the catalytic contributions of conserved active site residues in pfMDH. Our investigation further supports the currently accepted reaction mechanism. In addition, we discovered that the majority of residues in the pfMDH active site impart a greater contribution to its turnover rate than the Michaelis constant.

Materials and Methods

General materials

D–mannitol (Catalog #: 423922500) was purchased from Fisher. D–arabitol (Catalog #: A3381) and meso-erythritol (Catalog #: E7500) were purchased from Sigma-Aldrich. 1,2-Hexanediol (Catalog #: H0688) was purchased from TCI America. 1,2,3-Hexanetriol (Catalog #: H27180) was purchased from Alfa Aesar. All other buffers and reagents were purchased from Sigma-Aldrich or Fisher.

Construction of pfMDH gene

The gene coding for pfMDH derived from *Pseudomonas fluorescens* was synthesized by Invitrogen Life Technologies, GeneArt, and codon optimized for *Escherichia coli* as a DNA String (DNA and amino acid sequence provided in Supporting Information Fig. S1). The string was cloned into the pET-29b(+) plasmid vector using the Gibson assembly method between the NdeI and XhoI restriction sites.[25] A C-terminal 6x-His tag was genetically encoded for affinity column purification with HisPur cobalt beads. The resulting plasmid was sequence verified and transformed into electrocompetent BLR(DE3) strain *Escherichia coli* obtained from Novagen for protein expression.

Mutagenesis, expression, and purification of pfMDH

Site-directed mutagenesis was performed according to the protocol developed by Kunkel to introduce the mutations into the pfMDH gene and confirmed by DNA sequencing.[26] Ice scrapes of previously grown of BLR(DE3) cells transformed with pET-29b(+) plasmids containing the genes for WT and mutant pfMDH were used to inoculate 2 mL of Terrific Broth II from MP Biomedicals containing 50 μg/mL kanamycin. The 2 mL cultures were grown for 12 hours at 37°C and were diluted in 500 mL of Terrific Broth II. Diluted cultures were grown at 37°C for 24 hours and were pelleted by centrifugation at 4700 rpm for 30 minutes. Cell pellets were resuspended in 500 mL of auto-induction media and were grown for 30 hours at 18°C for the overexpression of protein. Cells were centrifuged for 30 minutes at 4700 rpm for collection. To lyse, the collected cell pellets were resuspended in 40 mL 1x PBS (pH 7.4), 1 mg/mL Lysozyme, 0.1 mg/mL DNase, and 0.1 m*M* PMSF. A Fisher Scientific Model 705 sonic dismembrator was used to sonicate and lyse the resuspended cells. The sonicator was set to amplitude 30 and the total sonication time for resuspended cells was 2 minutes: cells were sonicated in four 30-second intervals with 1 minute in between sonications. Cells were on ice during the sonication process. Lysate was clarified by centrifugation at 4700 rpm for 30 minutes and was then passed through a 5 μm filter. Supernatant was passed through a gravity column containing 1 mL of 50% HisPur cobalt resin slurry and washed with 10 column volumes of 1x PBS composed of 137 m*M* NaCl, 2.7 m*M* KCl, 10 m*M* Na_2HPO_4, and 2 m*M* KH_2PO_4 (pH 7.4). Protein was eluted with two 1.5 mL washes of 200 m*M* imidazole in 1x PBS (pH 7.4). Protein concentrators (20 mL capacity, 5 K MWCO) were used to buffer exchange the proteins into 50 m*M* HEPES containing 150 m*M* NaCl (pH 7.4). Protein was loaded into the protein concentrator and was centrifuged at 4700 rpm until the protein was concentrated to 1 mL. The concentrated protein was diluted with 19 mL of 50 m*M* HEPES containing 150 m*M* NaCl (pH 7.4) and centrifuged at 4700 rpm until the protein was concentrated back to 1 mL. Protein was diluted and concentrated at least five times to switch the buffer from 1x PBS with 200 m*M* imidazole (pH 7.4) to 50 m*M* HEPES containing 150 m*M* NaCl (pH 7.4). Protein purity was confirmed on a Coomasie-stained SDS-PAGE gel and was assayed within 72 hours of purification.

Kinetic experiments

Activity of WT and mutant pfMDH was measured by the accumulation of NADH resulting from the oxidation of the assayed substrates. All assays were performed by incubating 0.09–4 μ*M* pfMDH enzyme with two-fold serially diluted substrate in a 100 μL reaction containing 50 m*M* HEPES (pH 7.4),

150 m*M* NaCl, 1 mg/mL bovine serum albumin (BSA) and 1 m*M* NAD^+.

The addition of BSA prevented the adsorption of pfMDH onto the 96-well plates used in the assays. Proteins were equilibrated to room temperature for 10 minutes before assays were performed. Assays were initiated through the addition of 10 μL enzyme to 90 μL of 50 m*M* HEPES (pH 7.4) containing 150 m*M* NaCl, 1.11 mg/mL BSA and 1.11 m*M* NAD^+. The change in absorbance of NADH at a wavelength of 340 nm was measured using Biotek Epoch and Synergy microplate spectrophotometers. Kinetic constants were derived from the steady-state velocity curves using R (Regression plots available in Supporting Information Figs. S2–S4).

To perform the glycerol inhibition assay, 10 μL of glycerol at various concentrations were added to 80 μL of 50 m*M* HEPES containing 150 m*M* NaCl, 1 mg/mL BSA, 1 m*M* NAD^+, and 1 μ*M* WT pfMDH across columns in a 96-well plate. The assay was initiated with 10 μL of D–mannitol at various concentrations down the rows of the 96-well plate and the evolution of NADH was recorded by measuring the change in absorbance at a wavelength of 340 nm. The final concentrations of D–mannitol were 5, 50, and 500 m*M* and the final concentrations of glycerol were 0%, 0.1%, 1%, and 10% (v/v).

Acknowledgment

We would like to thank Dr. David Wilson for insightful discussions regarding the pfMDH structure and mechanism. This study was supported by funding from UC Davis.

References

1. Slatner M, Nidetzky B, Kulbe KD (1999) Kinetic study of the catalytic mechanism of mannitol dehydrogenase from *Pseudomonas fluorescens*. Biochemistry 38:10489–10498.
2. Benkovic SJ, Hammes-Schiffer S (2003) A perspective on enzyme catalysis. Science 301:1196–1202.
3. Mulholland AJ (2005) Modelling enzyme reaction mechanisms, specificity and catalysis. Drug Discov Today 10:1393–1402.
4. Klimacek M, Kavanagh KL, Wilson DK, Nidetzky B (2003) On the role of Bronsted catalysis in *Pseudomonas fluorescens* mannitol 2-dehydrogenase. Biochem J 375:141149.
5. Klimacek M, Nidetzky B (2002) Examining the relative timing of hydrogen abstraction steps during NAD(+)-dependent oxidation of secondary alcohols catalyzed by long-chain D–mannitol dehydrogenase from *Pseudomonas fluorescens* using pH and kinetic isotope effects. Biochemistry 41:10158–10165.
6. Klimacek M, Nidetzky B (2010) From alcohol dehydrogenase to a "one-way" carbonyl reductase by active-site redesign: A mechanistic study of mannitol 2-dehydrogenase from *pseudomonas fluorescens*. J Biol Chem 285:30644–30653.
7. Klimacek M, Kavanagh KL, Wilson DK, Nidetzky B (2003) *Pseudomonas fluorescens* mannitol 2-dehydrogenase and the family of polyol-specific long-chain dehydrogenases/reductases: Sequence-based classification and analysis of structure–function relationships. Chem Biol Interact 143–144:559–582.
8. Bubner P, Klimacek M, Nidetzky B (2008) Structure-guided engineering of the coenzyme specificity of *Pseudomonas fluorescens* mannitol 2-dehydrogenase to enable efficient utilization of NAD(H) and NADP(H). FEBS Lett 582:233–237.
9. Klimacek M, Nidetzky B (2010) The oxyanion hole of *Pseudomonas fluorescens* mannitol 2-dehydrogenase: A novel structural motif for electrostatic stabilization in alcohol dehydrogenase active sites. Biochem J 425:455–463.
10. Hammes GG, Benkovic SJ, Hammes-Schiffer S (2011) Flexibility, diversity, and cooperativity: Pillars of enzyme catalysis. Biochemistry 50:10422–10430.
11. Kavanagh KL, Klimacek M, Nidetzky B, Wilson DK (2003) Crystal structure of *Pseudomonas fluorescens* mannitol 2-dehydrogenase: Evidence for a very divergent long-chain dehydrogenase family. Chem Biol Interact 143–144:551–558.
12. Kearse M, Moir R, Wilson A, Stones-Havas S, Cheung M, Sturrock S, Buxton S, Cooper A, Markowitz S, Duran C, Thierer T, Ashton B, Meintjes P, Drummond A (2012) Geneious Basic: An integrated and extendable desktop software platform for the organization and analysis of sequence data. Bioinformatics 28:1647–1649.
13. Miller G (2002) Drug targeting. Breaking down barriers. Science 297:1116–1118.
14. Jaques A, Daviskas E, Turton JA, McKay K, Cooper P, Stirling RG, Robertson CF, Bye PT, Lesouef PN, Shadbolt B, Anderson SD, Charlton B (2008) Inhaled mannitol improves lung function in cystic fibrosis. Chest 133:1388–1396.
15. Kim AI, Akers MJ, Nail SL (1998) The physical state of mannitol after freeze-drying: Effects of mannitol concentration, freezing rate, and a noncrystallizing cosolute. J Pharm Sci 87:931–935.
16. Kearsley MW, Deis RC. Sorbitol and Mannitol, in Sweeteners and Sugar Alternatives in Food Technology. In Mitchell H, Ed. (2006) Oxford, UK: Blackwell Publishing Ltd. doi: 10.1002/9780470996003.ch13
17. Klimacek M, Nidetzky B (2002) A catalytic consensus motif for D–mannitol 2-dehydrogenase, a member of a polyol-specific long-chain dehydrogenase family, revealed by kinetic characterization of site-directed mutants of the enzyme from *Pseudomonas fluorescens*. Biochem J 367:13–18.
18. Kavanagh KL, Klimacek M, Nidetzky B, Wilson DK (2002) Crystal structure of *Pseudomonas fluorescens* mannitol 2-dehydrogenase binary and ternary complexes. Specificity and catalytic mechanism. J Biol Chem 277:43433–43442.
19. Finn RD, Clements J, Eddy SR (2011) HMMER web server: Interactive sequence similarity searching. Nucleic Acids Res 39:W29–W37.
20. Magrane M, Consortium U (2011) UniProt Knowledgebase: A hub of integrated protein data. Database 2011:bar009.
21. Huang Y, Niu B, Gao Y, Fu L, Li W (2010) CD-HIT Suite: a web server for clustering and comparing biological sequences. Bioinformatics 26:680–682.
22. Edgar RC (2004) MUSCLE: multiple sequence alignment with high accuracy and high throughput. Nucleic Acids Res 32:1792–1797.

23. Sheu SY, Yang DY, Selzle HL, Schlag EW (2003) Energetics of hydrogen bonds in peptides. Proc Natl Acad Sci USA 100:12683–12687.
24. Pace CN (2009) Energetics of protein hydrogen bonds. Nat Struct Mol Biol 16:681–682.
25. Gibson DG, Young L, Chuang RY, Venter JC, Hutchison CA, 3rd, Smith HO (2009) Enzymatic assembly of DNA molecules up to several hundred kilobases. Nat Meth 6:343345.
26. Kunkel TA (1985) Rapid and efficient site-specific mutagenesis without phenotypic selection. Proc Natl Acad Sci USA 82:488–492.
27. Schrodinger LLC (2010) The PyMOL Molecular Graphics System, Version 1.3r1.